JOURNAL OF Materials CHEMISTRY

# Synthesis of new MCM-36 derivatives pillared with alumina or magnesia–alumina

**Jan-Olaf Barth, Jan Kornatowski and Johannes A. Lercher***

*Lehrstuhl II für Technische Chemie, Technische Universität München, Lichtenbergstraße 4, D-85747 Garching bei München, Germany. E-mail: johannes.lercher@ch.tum.de*

***Received 1st June 2001, Accepted 15th November 2001***
***First published as an Advance Article on the web 3rd January 2002***

Alumina and magnesia–alumina have been applied for pillaring the layered precursor of zeolite MCM-22. Calcination of such materials has led to new varieties of MCM-36 molecular sieves. Pillaring with alumina yields mesoporous materials with lower surface areas than those pillared with silica. The pillaring process with alumina strongly depends upon the preparation conditions of the alumina species and requires an elongated aging of the pillaring solutions. Application of magnesia in addition to alumina results in a higher exfoliation of the MCM-22 layers and incorporation of an increased amount of alumina into the materials. $MgO \times Al_2O_3$ as pillaring agent yields a significantly higher mesoporosity in the range of 2–4 nm as compared with $Al_2O_3$. This synthesis method is a promising tool for tailoring the physicochemical properties and the structure of the slit-mesopores in relation to materials typically pillared with silica.

## Introduction

The MCM-36 structure combines zeolitic microporosity with mesoporosity originating from swelling of a layered precursor and pillaring the layers with $SiO_2$ species formed into larger polymeric units. This modification makes the material promising for potential applications as a catalyst or sorbent.[1,2] The synthesis procedure by Roth *et al.*[3–5] involves three steps: (i) hydrothermal synthesis of the layered MCM-22 precursor, (ii) swelling of the non-calcined MCM-22 precursor with hexadecyltrimethylammonium cations resulting in significantly increased distances between the zeolitic sheets, and (iii) pillaring (intercalation) of the sheets with $SiO_2$ oligomers formed *via* hydrolysis of TEOS (tetraethoxysilane) introduced into the suspension of the swollen precursor. This material is calcined, which results in the stabilization of the intercalated sheets and the removal of organic swelling compounds from the pores. The mesopores have the form of two-dimensional, regularly spaced slits between zeolitic layers. Thus, the mesopores are similar to the slit pores in pillared clays, while the layers have a strongly corrugated structure. Such a pillaring procedure does not yield mesopores of perfectly regular size as, for example, in the MCM-41 type materials. However, the interlayer distances depend upon the process of swelling and formation of the intercalating pillars, *i.e.* in broad sense, on the synthesis conditions. In this light, the transformation procedure implies that materials of this type can also be created by pillaring with use of compounds other than $SiO_2$.[4] Depending upon the compounds used for pillaring, such modification can result in tailoring or varying the acid–base[6–8] and ion-exchange properties[7–9] as well as the dimensions/structure of the slit-mesopores.[8] The new features, and especially the high specific surface area and good accessibility for larger molecules, may expand the range of catalytic applications. Here, we report on the synthesis of MCM-36 materials pillared with two alumina-containing species, *i.e.* $Al_2O_3$ and $MgO \times Al_2O_3$.

## Experimental

### Synthesis

The MCM-22 precursor was synthesized according to the procedure described by Rubin and coworkers[10] and modified by He *et al.*[2,11] with the only difference that the hydrothermal crystallization proceeded under static conditions without stirring/rotating the autoclaves. The reaction gel was prepared from Aerosil 200 (Degussa), $NaAlO_2$ [Riedel de Haen; 44.8% Na (as $Na_2O$), 55.2% Al (as $Al_2O_3$)], NaOH (Fluka), hexamethyleneimine (HMI, 99%, Merck), and deionized water in molar ratios (as oxides) 1 : 0.1 : 0.2 : 0.5 : 40, respectively. The gel was placed in PTFE-lined autoclaves and heated statically at 423 K for 10 days. The resulting solid, which is the precursor of MCM-22, was divided into two portions. One of them was filtered, washed with water, dried at room temperature in air and finally calcined at 823 K under flowing $N_2$ with 8% $O_2$ for 48 h to produce crystalline MCM-22 zeolite. The other portion of the precursor was used for the synthesis of the MCM-36 materials by swelling and pillaring with alumina, magnesia–alumina, and $SiO_2$ (reference material).

The swelling process, identical for all samples, was performed following the procedure described by He *et al.*[2] A wet cake of MCM-22 (containing 25–30 wt.% MCM-22 precursor in $H_2O$) was mixed with hexadecyltrimethylammonium chloride (CTMACl, Fluka; 25% solution in $H_2O$) and tetrapropylammonium hydroxide (TPAOH, Heraeus; 20% solution in $H_2O$) at a weight ratio of 1 : 4 : 1.2, respectively. The pH of the mixture was adjusted to 13.5 with 0.1 M NaOH. The mixture was then heated at 373 K under continuous stirring for 68 h and subsequently agitated at room temperature for 4 h. The resulting swollen material was filtered, washed with a small amount of water, and dried at ambient conditions.

The solutions for pillaring with alumina were prepared as follows: 720 ml of a 0.2 M NaOH (Fluka) solution was dropwise added to 720 ml of 0.1 M $AlCl_3$ (Merck) solution under stirring. The mixture was agitated at 363 K for 4 h and finally aged at 298 K for 15 or 60 h for preparing samples A and B (Tables 1 and 2).[12] For pillaring with $MgO \times Al_2O_3$, to the same Al solution as above (after aging for 60 h), 1.45 g MgO (Aldrich) was slowly added under stirring (molar ratio $Mg : Al : OH = 1 : 2 : 4$) and the resulting mixture was agitated at room temperature overnight.

Pillaring was performed by adding a 10 wt.% water suspension of 3 g of the swollen MCM-22 precursor to the pillaring solution (*ca.* 24 mmol Al/g swollen MCM-22 precursor). The mixture was heated at 353 K under stirring

DOI: 10.1039/b104824b

**Table 1** Structural properties of calcined MCM-22/36 samples

| Sample | BET surface area/$m^2\ g^{-1}$ | Micropore surface area/$m^2\ g^{-1}$ | Macro-/meso-pore surface area/$m^2\ g^{-1}$ | Micropore volume/ $cm^3\ g^{-1}$ | BJH mesopore size distribution (maximum)/Å |
|---|---|---|---|---|---|
| MCM-22 | 432 | 324 | 108 | 0.155 | — (—) |
| $SiO_2$-MCM-36 | 710 | 321 | 389 | 0.044 | 15–35 (22) |
| $Al_2O_3$-MCM-36 (sample A) | 380 | 126 | 254 | 0.022 | 15–38 (25) |
| $Al_2O_3$-MCM-36 (sample B) | 357 | 156 | 201 | 0.065 | 17–38 (17) |
| MgO × $Al_2O_3$-MCM-36 | 348 | 93 | 255 | 0.018 | 17–40 (24) |

**Table 2** Elemental composition of MCM-22/36 samples (determined from AAS analysis; for MgO × $Al_2O_3$-MCM-36 from EDX surface analysis)

| Sample | Si : Al (AAS) | Si : Al (EDX) | Si (wt.%) | Al (wt.%) | Na (wt.%) | Mg (wt.%) |
|---|---|---|---|---|---|---|
| MCM-22 | 11.37 | 10.56 | 45.40 | 3.85 | 0.25 | — |
| $SiO_2$-MCM-36 | 28.46 | 28.70 | 43.38 | 1.47 | <0.10 | — |
| $Al_2O_3$-MCM-36 (sample A) | 5.92 | 8.11 | 40.22 | 6.55 | 0.90 | — |
| $Al_2O_3$-MCM-36 (sample B) | 6.23 | 6.21 | 36.49 | 5.65 | <0.10 | — |
| MgO × $Al_2O_3$-MCM-36 | — | 1.26 | 27.92 | 21.28 | <0.10 | 0.64 |

for 25 h. The products were filtered, dried at room temperature overnight and calcined at 673 K (ramp 1 K $min^{-1}$) under $N_2$ flow (100 ml $min^{-1}$) for 6 h, and subsequently at 823 K (ramp 2 K $min^{-1}$) under synthetic air (100 ml $min^{-1}$) for 12 h.[6]

For pillaring of the reference MCM-36, the swollen MCM-22 was mixed with TEOS (tetraethoxysilane, Merck) at a weight ratio of 1 : 5, heated at 351 K under $N_2$ with stirring for 25 h, then filtered and dried at room temperature. The resulting solid was hydrolyzed at 313 K as suspension in water (wt. ratio 1 : 10) of pH = 8 (controlled with NaOH) for 6 h, then filtered, dried at 300 K, and calcined at 723 K under $N_2$ flow (30 ml $min^{-1}$) for 6 h and finally at 823 K under air for 12 h.

### Characterization

Powder X-ray diffraction patterns were collected to estimate crystallinities and the structural changes of the synthesized materials on a Philips X'Pert-1 System diffractometer using Cu-Kα radiation ($\lambda$ = 1.54186 Å). Data were collected in the $2\theta$ range from 5 to 50° with a step size of 0.02° and a step time of 5 s. Low-angle XRD measurements were performed with a Huber G653 device, collecting data in the $2\theta$ range from 0.5 to 10° with a step size of 0.02° and a step time of 5 s.

Elemental analyses were obtained using atomic adsorption spectroscopy (AAS) with a UNICAM 939 AA-Spectrometer. Energy dispersive X-ray fluorescence (EDX) measurements were carried out using a JEOL 500 scanning electron microscope equipped with a Röntec EDX-spectrometer.

Nitrogen adsorption measurements were performed at 77.4 K with a PMI Automated BET sorptometer 5.32. The samples were degassed at 673 K and $10^{-3}$ Pa for 24 h prior to the adsorption measurements. The specific surface areas were calculated by the Brunauer–Emmet–Teller (BET) method. The mesopore size distributions were obtained from the desorption branch of the isotherm. The pore size distribution was calculated using the Barret–Joyner–Halenda (BJH) method.[13] Concerning the results of the pore size determination it has to be taken into account that the BJH method has been shown to systematically underestimate the pore size and that there have been several attempts to solve this problem.[14–16] However, the BJH method is usually applied in the literature as the standard method for comparing mesopore sizes.[17–19] In the present study we make use of this method to facilitate a better comparison of the pore size distributions typical of our samples. The micropore volume was calculated from *t*-plots using the Harkins–Jura equation.

The morphologies and crystal sizes of the synthesized materials were examined by scanning electron microscopy (SEM, JEOL 500) at an accelerating voltage of 25 kV. The samples were sputtered with gold before taking the images.

For transmission electron microscopy (TEM), the sample was suspended in isopropanol and adsorbed on a carbon-coated copper grid. After drying in air overnight, the sample was placed inside the microscope (JEOL 2010, operated at 200 kV, $LaB_6$ electron source) equipped with a 1024 × 1024 pixel cooled slow-scan CCD-camera (TVIPS, Gauting, Germany) and interfaced to a computer for microscope control and image acquisition.

## Results and discussion

XRD powder patterns (Fig. 1) correspond well to those reported in the literature[2–5,10,11,20] and the prepared solids have been identified as MCM-36 materials. As can be seen from Fig. 1, the expansion of the materials along the crystallographic *c*-axis caused a slight shift of *hkl* reflections while *hk0* reflections remain unchanged. For example, the positions of the prominent narrow peaks 100, 220, and 310 at $2\theta$ = 7.2°, 25.1°, and 26.1° ($2\theta$, Cu-Kα) respectively, are unaffected. The patterns of the pillared materials displayed a broad peak at *ca.* 10°, which may be the result of a broadening of the 102 reflection due to a loss of layer ordering in the *c*-direction.[20] The reflections 001 at 3.2° (not shown) and 002 at 6.5° of the MCM-22 precursor correspond to the unit cell *c*-parameter of 27 Å and disappear upon pillaring. The new *c*-parameter of the $SiO_2$ pillared MCM-36 material is reflected in an intense and broad low-angle peak at 1.6° (Fig. 2) corresponding to a *d*-spacing of *ca.* 50 Å. For all samples, the low-angle peaks show an asymmetric shape with a less defined background at the side of higher $2\theta$. We attribute this effect to a distribution of *d*-spacings within the range between 30 and 50 Å. Both, the alumina and magnesia–alumina, pillared materials show an

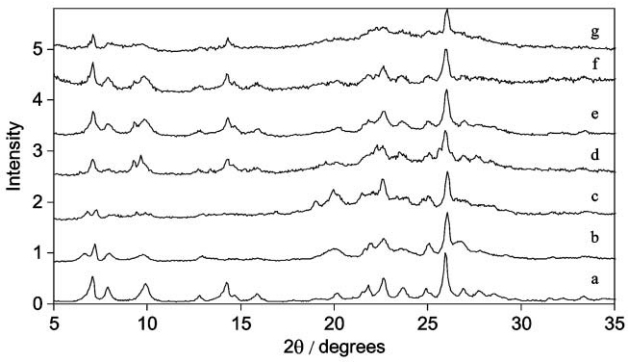


**Fig. 1** Powder X-ray diffraction patterns of (a) MCM-22, calcined; (b) MCM-22, as-prepared; (c) MCM-22, swollen; (d) $Al_2O_3$-MCM-36 (sample A); (e) $Al_2O_3$-MCM-36 (sample B); (f) MgO × $Al_2O_3$-MCM-36; and (g) $SiO_2$-MCM-36.

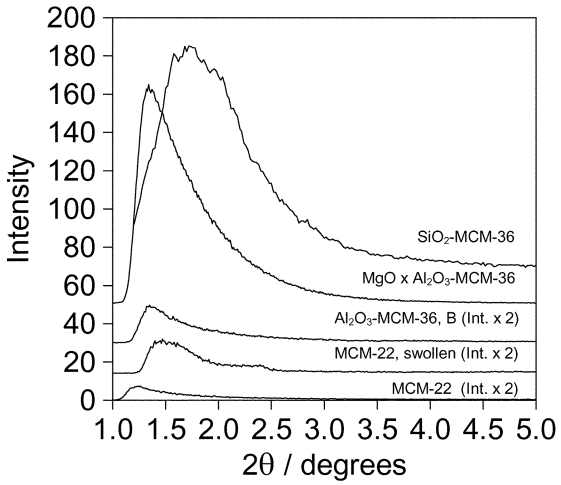


**Fig. 2** Low-angle powder X-ray diffraction patterns of MCM-22, calcined; MCM-22, swollen; $Al_2O_3$-MCM-36 (sample B); MgO × $Al_2O_3$-MCM-36; and $SiO_2$-MCM-36.

additional new peak of unknown origin at 9.4° (Fig. 1), which might be attributed to 00*l* reflections of higher order. For both materials, interlayer distances calculated by subtracting the thickness of the MCM-22 layer (2.5 nm) from the *d*-values are equal to 0.5–2.5 nm. They indicate that swelling and pillaring with alumina and magnesia–alumina do not cause formation of pores and galleries of regular shapes and sizes. This observation is supported by the mesopore size distributions (BJH method, Fig. 3), which reveal mesopores within the range of 2–4 nm.

The AAS analysis results (Table 2) show that the Si : Al ratio strongly increases as the result of transformation from MCM-22 to $SiO_2$-MCM-36 (11.4 and 28.5, respectively), which indicates an intercalation of $SiO_2$ moieties between the MCM-22 layers and a dealumination during the pillaring process. As opposed to that, the Si : Al ratio decreases strongly to *ca.* 6 upon pillaring with the alumina species, which indicates a high amount of alumina retained in the solid material. As all three alumina pillared materials show a higher crystallinity than $SiO_2$-MCM-36 (XRD, Fig. 1), it is difficult to assess the effect of these pillaring species on a possible dealumination. The AAS analysis gives no reliable results for Si in MgO × $Al_2O_3$-MCM-36, as this material is hardly soluble. Based on EDX surface analysis, the Si : Al ratio decreases significantly to *ca.* 1.3 indicating a strongly increased concentration of Al in the sample. The Al : Mg ratio equals ≈29.6 suggesting a relatively low incorporation of MgO into the material.

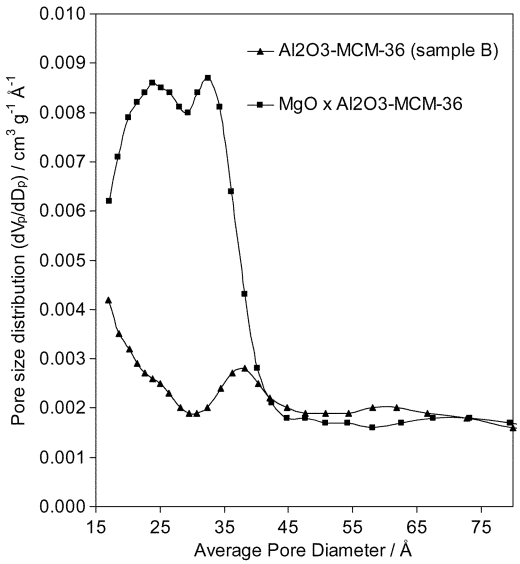


**Fig. 3** Mesopore size distribution (BJH-method) determined from nitrogen adsorption.

The conclusions from XRD agree well with the changes in morphology observed by SEM (Fig. 4). MCM-22 forms a uniform phase of disc-like aggregates of zeolitic platelets. The $SiO_2$ pillared MCM-36 sample exhibits irregular particles of agglomerated layers (swollen platelet structure[2]) and pillaring with the alumina species results in stronger changes in morphology. The sample A pillared with $Al_2O_3$ points out a partial, whereas the sample B indicates a full transformation of the crystallites characteristic of the MCM-22 precursor. The sample pillared with MgO × $Al_2O_3$ is composed (*cf.* Fig. 4e) of small particles of various shapes and dimensions and does not show remains of the typical MCM-22 morphology. This agrees well with the fact that the XRD pattern of this material indicates the highest degree of 'amorphization' among the alumina pillared samples. These observations are supported by results of the EDX analysis. For MCM-22 and $SiO_2$-MCM-36, consistent concentrations of Si and Al were determined over the whole sample analysed by SEM, indicating a high degree of purity. $Al_2O_3$-MCM-36 (sample A) still shows remains of the MCM-22 precursor with a Si : Al ratio of *ca.* 11.2, *i.e.* similar to MCM-22. The transformed part of the material, with irregular particle morphology, exhibits a Si : Al ratio of 6.0. For $Al_2O_3$-MCM-36 (sample B), an almost full transformation was achieved, which is in agreement with the obtained Si : Al ratios determined by EDX (6.2) and AAS (6.2). MgO × $Al_2O_3$-MCM-36 is composed of particles of various shapes and sizes and hardly resembles the MCM-22 morphology. The Si : Al ratio (*ca.* 1.3) determined from EDX analysis indicates that the predominant amount of Al used for the pillaring treatment has been retained in the material. Interestingly, a small fraction of particles of larger dimensions exhibits an even lower Si : Al ratio (0.7), which suggests that such large particles concentrate more Al on their external surface. These phenomena have not been observed for the materials pillared without MgO. Although

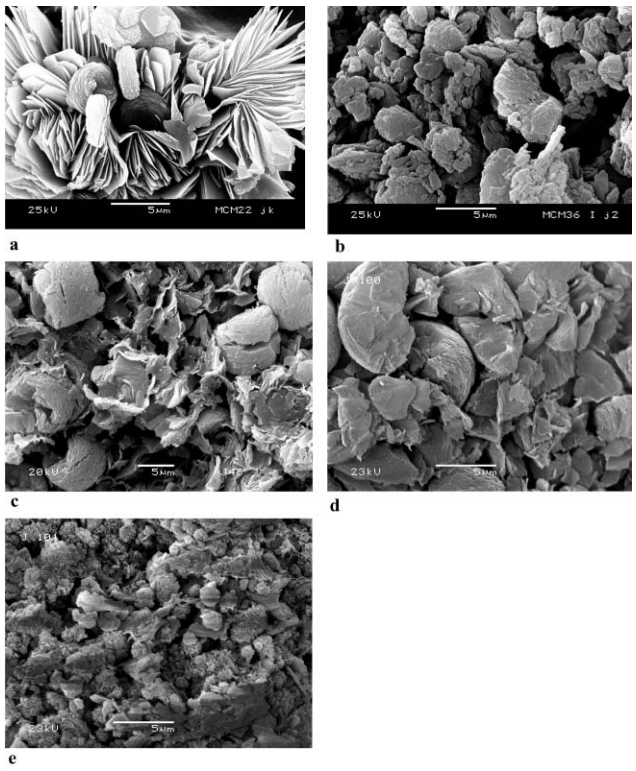


**Fig. 4** Scanning electron micrographs of (a) MCM-22, calcined; (b) $SiO_2$-MCM-36; (c) $Al_2O_3$-MCM-36 (sample A); (d) $Al_2O_3$-MCM-36 (sample B); and (e) MgO × $Al_2O_3$-MCM-36.

both, AAS and EDX analysis, indicate only a low amount of incorporated Mg (0.64 wt.%), a strong influence of magnesia on the pillaring process is seen.

TEM micrographs (Fig. 5 shows an example of MgO × $Al_2O_3$-MCM-36) demonstrate clearly that the materials have a well resolved layer structure. The pillared zeolite sheets form aggregates of *ca.* 100–150 nm length and *ca.* 100 nm width. The layer thickness can be estimated to be *ca.* 2.5 nm which is consistent with the values reported by Roth *et al.*[3,20] The presence of pillars keeping the layers apart cannot be observed directly probably due to insufficient contrast. These less dense areas between the sheets are attributed to interlayer distances being equal to *ca.* 0.1 nm (Fig. 5 right). The packing of the MCM-22 sheets seems to be less regular on the borders and the outer termination of the aggregates (Fig. 5 left).

Fig. 6 shows the nitrogen adsorption–desorption isotherms of MgO × $Al_2O_3$-MCM-36 and $Al_2O_3$-MCM-36 (sample B) compared with those of zeolite MCM-22. The sorption isotherm of zeolite MCM-22 (unpillared reference material) corresponds to a Type I isotherm in the Brunauer, Deming, Deming and Teller (BDDT) classification, indicating the presence of microporosity.[21] The sorption isotherms of the pillared materials correspond to Type II isotherms referring both to micro- and mesoporosity. The shift towards mesoporosity is more pronounced for MgO × $Al_2O_3$-MCM-36 as compared to $Al_2O_3$-MCM-36. The hysteresis loops correspond to Type H3 in the IUPAC classification[22] and B-type according to de Boer.[23] H3-type isotherms are typical for materials having slit-shaped pores and plate-like particles with spaces between the parallel plates.[22–24] The form of the presented isotherms demonstrates a layered structure in the MCM-36 derivatives. This is consistent with the expected structure of materials prepared by expanding a layered zeolitic precursor.

Fig. 3 shows the mesopore size distribution (BJH method) of MgO × $Al_2O_3$-MCM-36 and $Al_2O_3$-MCM-36 (sample B). Using the binary oxide MgO × $Al_2O_3$ as pillaring agent yields a significantly higher mesoporosity in the range of 20–40 Å as compared to $Al_2O_3$ (*cf.* Table 1). Mesoporosity of MCM-36 originates from two processes during the calcination procedure: (i) dehydration of polycationic Al precursors in the pillaring solution leads to the formation of stable oxidic clusters/pillars and a linking of them to the zeolite layers (accompanied by the formation of stacking defects); (ii) the organic swelling molecules ($CTMA^+$, TPAOH) are removed simultaneously from the interlayer spaces leaving voids. Obviously, mixed alumina oxides like MgO × $Al_2O_3$ form larger and thermally more stable pillars (preventing a collapse

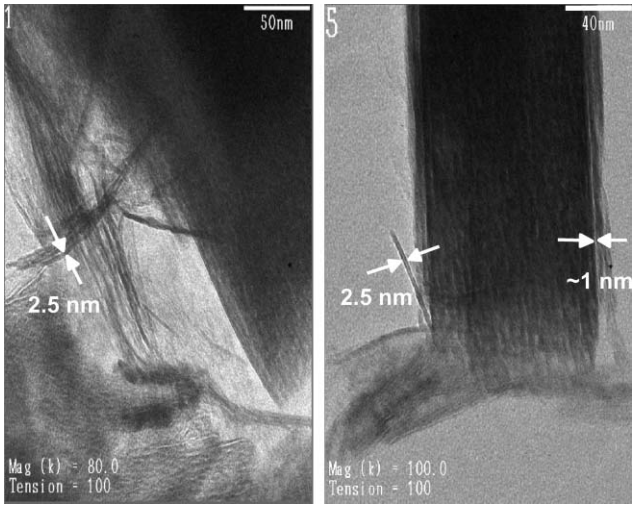


**Fig. 5** Transmission electron micrographs of MgO × $Al_2O_3$-MCM-36 [magnification 80k (left), 100k (right)].

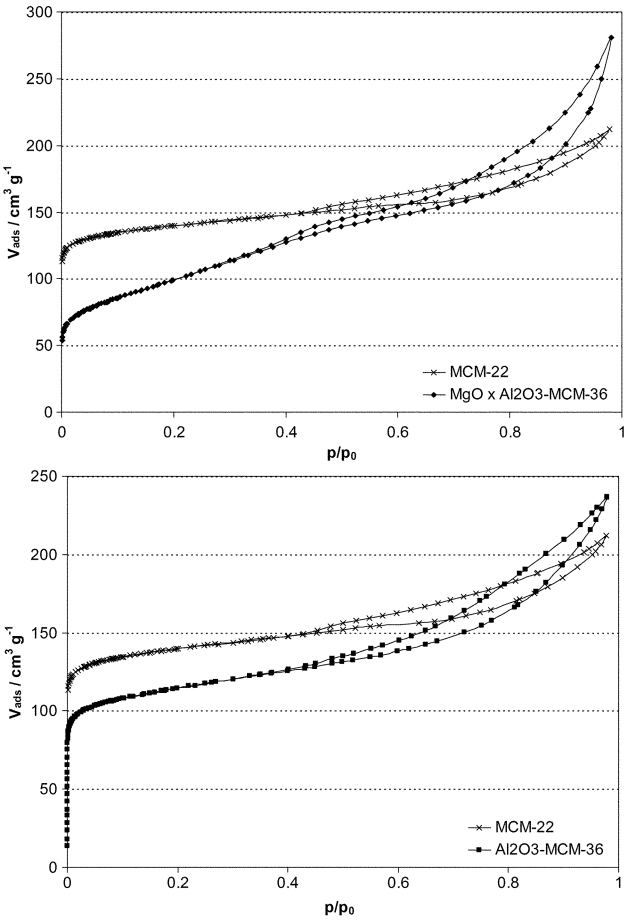


**Fig. 6** Nitrogen adsorption–desorption isotherms of (top) MgO × $Al_2O_3$-MCM-36 and (bottom) $Al_2O_3$-MCM-36 (sample B) compared with MCM-22.

of the pillared structure during calcination) as compared to pure $Al_2O_3$. This requires a further examination.[25] The narrow shape of the pore size distribution indicates that a homogeneous structure is formed in the interlayer region of the MCM-36 derivatives described here.

The differences between the two $Al_2O_3$ pillared samples are attributed to the formation of Al polyoxocations, the Keggin units $[Al_{13}O_4(OH)_{24}(H_2O)_{12}]^{7+}$, necessary for the pillaring process. Hydrolysis of $AlCl_3$, *i.e.* aging of the Al species solutions for pillaring, was made for 15 and 60 h for the samples A and B, respectively. The presented results are in line with the report of Canizares *et al.*[6] that the formation of the Keggin units requires an elongated aging of the Al pillaring solutions and that 20 h is most likely the minimum necessary period.

## Conclusions

The precursor of zeolite MCM-22 can be synthesized under static conditions without agitation of the reaction mixture. The material prepared in this way can be exfoliated and transformed into MCM-36, similarly to precursors synthesized under rotating conditions. Pillared MCM-36 can be successfully synthesized by an appropriate treatment of the MCM-22 precursor with alumina and magnesia–alumina species. Pillaring with alumina appears to be effective and yields mesoporous materials with lower surface areas than those pillared with silica. The pillaring with alumina strongly depends on the preparation conditions of the alumina species and requires an elongated aging of the solutions used for the pillaring process, *i.e.* to form Keggin units of appropriate size. Application of magnesia in addition to alumina results in a higher exfoliation

of the MCM-22 precursor and incorporation of an increased amount of alumina into the pillared materials. This suggests a significant role of the basic oxide MgO during the pillaring process.

Alumina and magnesia–alumina pillared MCM-36 show high mesoporosity combined with zeolitic microporosity.

## Acknowledgements

Financial support of the European Union (Project G1RD-CT99-0065-'DENOXPRO') is gratefully acknowledged. Special thanks go to Dr L. Simon (TUM Munich) for measuring the TEM micrographs. The authors are thankful to Dipl.-Ing. (FH) F.-X. Hecht and Dipl.-Ing. (FH) M. Neukamm for measuring nitrogen adsorption isotherms and AAS elemental analysis.

## References

1 C. T. Chu, H. Altaf, A. N. J. Huss, C. T. Kresge and W. J. Roth, *US Pat.*, 5 258 569, 1993.
2 Y. J. He, G. S. Nivarthy, F. Eder, K. Seshan and J. A. Lercher, *Microporous Mesoporous Mater.*, 1998, **25**, 207.
3 W. J. Roth, C. T. Kresge, J. C. Vartuli, M. E. Leonowicz, A. S. Fung and S. B. McCullen, *Stud. Surf. Sci. Catal.*, 1995, **94**, 301.
4 C. T. Kresge, W. J. Roth, K. G. Simmons and J. C. Vartuli, *US Pat.*, 5 229 341, 1993.
5 C. T. Chu, C. T. Kresge, W. J. Roth, K. G. Simmons and J. C. Vartuli, *US Pat.*,5 292 698, 1994.
6 P. Canizares, J. L. Valverde, M. R. Sun Kou and C. B. Molina, *Microporous Mesoporous Mater.*, 1999, **29**, 267.
7 J.-O. Barth, R. Schenkel, J. Kornatowski and J. A. Lercher, *Stud. Surf. Sci. Catal.*, 2001, **135**, 136.
8 A. Gil and L. M. Gandía, *Catal. Rev. Sci. Eng.*, 2000, **42**, 145.
9 R. T. Yang, N. Tharappiwattananon and R. Q. Long, *Appl. Catal., B*, 1998, **19**, 289.
10 M. E. Leonowicz, J. A. Lawton, S. L. Lawton and M. K. Rubin, *Science*, 1994, **264**, 1910; M. K. Rubin and P. Chu, *US Pat.*, 4 954 325, 1990.
11 F. Eder, Y. J. He, G. S. Nivarthy and J. A. Lercher, *Recl. Trav. Chim. Pays-Bas*, 1996, **115**, 531.
12 S. Schönherr, H. Görz, D. Müller and W. Gessner, *Z. Anorg. Allg. Chem.*, 1981, **476**, 188.
13 E. P. Barret, L. G. Joyner and P. P. Halenda, *J. Am. Chem. Soc.*, 1951, **73**, 373.
14 A. Galarneau, D. Desplantier, R. Dutartre and F. di Renzo, *Microporous Mesoporous Mater.*, 1999, **27**, 297.
15 M. Kruk, M. Jaroniec and A. Sayari, *Langmuir*, 1997, **13**, 6267.
16 W. W. Lukens, P. Schmid-Winkel, D. Zhao, J. Feng and G. D. Stucky, *Langmuir*, 1999, **15**, 5403.
17 N. D. Hutson, M. J. Hoekstra and R. T. Yang, *Microporous Mesoporous Mater.*, 1999, **28**, 447.
18 K. Sapag and S. Mendioroz, *Colloids Surf., A*, 2001, **141**, 187.
19 B. Lindlar, A. Kogelbauer, P. J. Kooyman and R. Prins, *Microporous Mesoporous Mater.*, 2001, **89**, 44.
20 W. J. Roth, J. C. Vartuli and C. T. Kresge, *Stud. Surf. Sci. Catal.*, 2000, **129**, 501.
21 S. Brunauer, L. S. Deming, W. S. Deming and E. Teller, *J. Am. Chem. Soc.*, 1940, **62**, 1723.
22 K. S. W. Sing, *Pure Appl. Chem.*, 1982, **54**, 2201.
23 J. H. de Boer, in *The Structure and Properties of Porous Materials*, ed. D. H. Everett and F. S. Stone, Butterworth, London, 1958, p. 68.
24 R. Mokaya and W. Jones, *J. Catal.*, 1995, **153**, 76.
25 J.-O. Barth, J. Kornatowski, A. Jentys and J. A. Lercher, to be published.